Original Article

Localization of in-stent neoatherosclerosis in relation to curvatures and bifurcations after stenting

Yongpeng Zou*, Xingtao Huang*, Linxing Feng, Jingbo Hou, Lei Xing, Bo Yu

Department of Cardiology, the 2nd Affiliated Hospital of Harbin Medical University, The Key Laboratory of Myocardial Ischemia, Chinese Ministry of Education, Harbin 150086, China

Contributions: (I) Conception and design: Y Zou, B Yu; (II) Administrative support: B Yu, J Hou; (III) Provision of study materials or patients: B Yu; (IV) Collection and assembly of data: Y Zou, X Huang; (V) Data analysis and interpretation: X Huang, L Feng; (VI) Manuscript writing: All authors; (VII) Final approval of manuscript: All authors.

*These authors contributed equally to this work.

Correspondence to: Bo Yu, MD, PhD. Department of Cardiology, the 2nd Affiliated Hospital of Harbin Medical University, The Key Laboratory of Myocardial Ischemia, Chinese Ministry of Education, Harbin 150086, China. Email: yubodr@163.com.

Background: In-stent neoatherosclerosis (ISNA) is a final common pathway of late-stent failure. However, distribution of ISNA has been little reported. This study was to evaluate the localization of ISNA in relation to curvatures and bifurcations after stent implantation using optical coherence tomography (OCT).

Methods: We retrospectively selected patients who underwent OCT examination ≥12 months after stent (sirolimus-eluting stents, SES) implantation. A stent curvature was defined if the angulation of the stent segment was >29°. Distribution of ISNA in relation to stent curvature and bifurcation was evaluated.

Results: Totally, 331 patients were enrolled. The mean follow-up time was 15 months. Forty-one (12.3%) patients were found with ISNA. OCT results showed that stents with ISNA had thicker neointima (mean neointima thickness: 0.16 *vs*. 0.08 mm, P<0.001) compared to patients without ISNA. Segments with angulation >29° had a higher prevalence of ISNA compared with to angulation ≤29° [18 (18.4%) *vs*. 23 (9.9%), P=0.032]. ISNA was more frequently located at the "inner curvature" than the "outer curvature" (77.8% *vs*. 22.2%, P=0.018). If ISNA occurred in a branch, it was more often on the opposite side of the branch compared with the same side of the branch [21 (77.8%) *vs*. 6 (22.2%), P=0.004].

Conclusions: Localization of ISNA is related to vessel curvatures and bifurcations. ISNA occurs more often on the inner curvature and the opposite side of the branch.

Keywords: Tomography; optical coherence; atherosclerosis; drug-eluting stents (DESs)

Submitted Jul 18, 2016. Accepted for publication Nov 03, 2016.
doi: 10.21037/jtd.2016.11.108
View this article at: http://dx.doi.org/10.21037/jtd.2016.11.108

Introduction

In-stent neoatherosclerosis (ISNA) has attracted much attention owing to its close association with late complications such as revascularization and late stent thrombosis (1-3). The incidence of ISNA was greater in drug-eluting stent (DES) than in bare metal stent (BMS) (3,4). Although the second-generation has been improved with more biocompatible polymers and thinner strut stent backbones than those with first-generation DES (5), it was not more protective against NA than the first-generation DES (6). It is important to understand the mechanisms of ISNA formation. Previous studies have found that one of the major mechanisms of ISNA was DES-induced endothelial dysfunction. However, there is litter study focus on the mechanical mechanism of ISNA formation, for example, the role of vessel anatomy. It is unknown that whether stent curvature and bifurcation site play a role in the formation and distribution of ISNA. In this study, we aimed to evaluate the localization of ISNA in relation to curvatures and bifurcations after SES implantation using OCT.

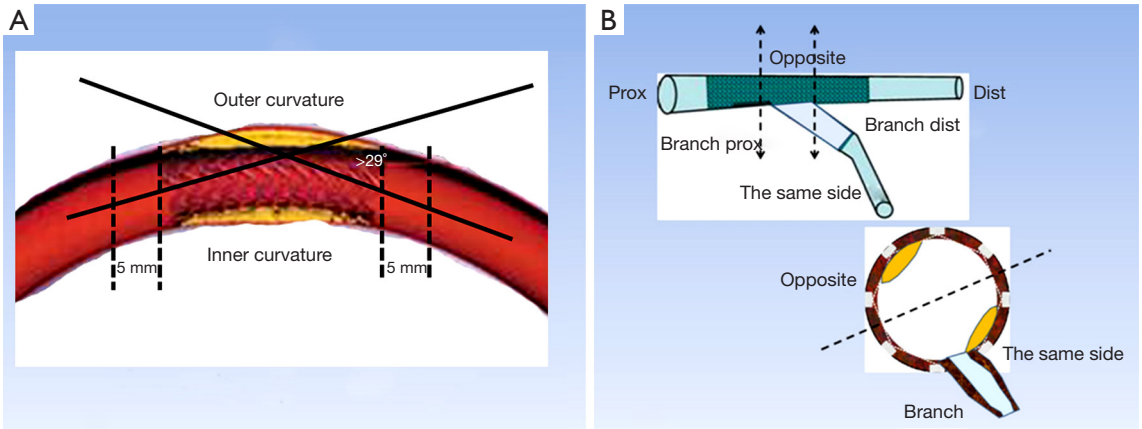

Figure 1 Illustration of curve definition and ISNA location. (A) The angulation of stent segment was defined as the angle formed by the tangents of the centerlines of the 5-mm proximal and distal parts of the segment. A curvature was defined if the angulation of the stent segment was >29°; (B) relationship between ISNA location and bifurcation position (schematic). Prox, proximal; Dist, distal.

Methods

Study population

This was a retrospective observation study. We retrospectively selected patients received single stent in single lesion and underwent OCT examination ≥12 months after stent (sirolimus-eluting stents, SES) implantation. The exclusion criteria in this study were as follows: (I) ST-segment elevation myocardial infarction; and (II) severe congestive heart failure. This protocol was approved by the Harbin Medical University Ethics Committee (No. KY-2015-105), and all patients received statins and antiplatelet therapy during the follow-up period.

Quantitative coronary angiography (QCA) analyses

QCA was undertaken by two independent investigators who were blinded to the clinical presentations. The intraobserver reliability of measurement results was confirmed by statistics. We selected an end-diastolic projection where there was minimal foreshortening view for the angle measurement. The angle measurement was performed using a programme installed in the QCA system (CASS version 5.10.1, Pie Medical Imaging BV, Maastricht, the Netherlands). The angulation of stent segment was defined as the angle formed by the tangents of the centerlines of the 5-mm proximal and distal parts of the segment (7). A stent curvature was defined if the angulation of the stent segment was >29° (*Figure 1*) (7). The branches posited at the inner curvature or outer curvature were marked to determine the position of ISNA in OCT images (*Figure 1*).

OCT examination

In this study, the data was collected from our OCT database according to our study criteria. Most of images were acquired by time-domain OCT system. Time-domain OCT with coronary artery occlusion was used as previously reported (4). In brief, a 0.4064 mm (0.016-inch) OCT catheter (ImageWire, LightLab Imaging, Westford, Massachusetts, USA) was advanced to the distal end of the stent through a 3-F occlusion balloon catheter. An occlusion balloon was inflated to 50.7–70.9 kPa (0.5–0.7 atm) at proximal site of the stent, lactate Ringer's solution was infused into the coronary artery from the distal tip of the occlusion balloon catheter at 0.5–2.0 mL/s by a high-pressure injector. The entire length of the stent was imaged with an automatic pullback device at 3 mm/s.

OCT images analysis

OCT images were analyzed by two independent investigators. If there was discordance in interpretations between the observers, a consensus reading was obtained by corresponding author. The intraobserver reliability of measurement results was confirmed by statistics. Cross-sectional OCT images were analyzed at 1-mm intervals along the pullbacks. Cross-sectional images were screened for quality assessment. If any portion of the image was outside the screen, if a side branch occupied >45° of the cross-section, or if the image was of poor quality due to residual blood, sew-up artifact, or reverberation, then it was excluded from the analysis. Lipid-laden neointimal was

defined as a diffusely bordered, signal-poor region with overlying signal-rich bands corresponding to fibrous caps (6). Calcification inside the neointimal was defined as a well-delineated, signal-poor region with sharp borders (6). Neointimal rupture was a break in the fibrous cap that connected the lumen with the underlying lipid pool (8). ISNA was defined as lesions with lipid-laden neointima, neointima with calcification, a thin-cap fibroatheroma-like neointima, or neointimal rupture (8,9).

To evaluate the relationship between ISNA location and vascular angle, we relocated the same branch as we had initially defined it on the angiogram (which helped identification of the inner curvature or outer curvature). Then, we observed the occurrence of ISNA at the inner curvature or outer curvature. A "relevant" branch was defined as a side branch with diameter >2 mm within 5 mm proximal or distal to the ISNA (10). According to the location of the relevant branch, we estimated the location of ISNA at the same side or opposite the branch, and proximal or distal to the branch (11).

To assess the relationship between ISNA location and side of the branch, patients with another side branch within 5 mm proximal or distal to the ISNA were excluded from OCT analyses.

Statistical analyses

Continuous variables are presented as mean ± SD or median values with inter-quartile range depending on their distributions. Categorical variables are presented using frequency counts and percentages. Continuous variables with normal distribution were analyzed with *t*-test and with nonparametric test (Mann-Whitney) for abnormal distributed ones. Categorical variables were compared using a chi-square test or Fisher's exact probability test, where appropriate. Intraclass correlation coefficient was used to confirm intraobserver reliability of measurement results. All analyses were carried out using SPSS v17.0 (SPSS, Chicago, IL, USA). For all comparisons a P value <0.05 was considered to represent a statistically significant result.

Results

Patient characteristics

A total of 331 patients were evaluated. Two hundred and eighty-eight patients came back for OCT examination without any symptom (Just for a CAG and OCT follow-up in order to finish the clinical trial, NCT01024179, NCT01023919, NCT01021930) and 43 patients back for unstable angina. Forty-one (12.3%) patients were found with ISNA, of which four patients occurred with unstable angina. The median duration of follow-up was 15 months. However, the patients with ISNA have much longer follow-up time which was 19 months compared to without ISNA patients (P<0.05). The clinical and procedural characteristics of patients were showed at *Table 1*.

Angiographic findings

There was no significant difference within intra-observer measurements (percent diameter stenosis: r=0.926, P<0.001; stent angle: r=0.975, P<0.001). The unstable angina occurred in four patients with ISNA turn out to be caused by target lesion in other vessel. Apparently, patients with ISNA have severe percent diameter stenosis compared to those without ISNA (22.8±5.23 *vs.* 15.6±4.22, P<0.001). However, there is no in-stent restenosis found in both groups. Combining with the results of OCT image, there was no significant difference in percentage of ISNA in different vessels. However, in the patients with ISNA have found more stents with an angulation >29° compared to patients without ISNA [18 (43.9%) *vs.* 80 (27.6%), P=0.032], which means stents with angulation >29° may had a higher prevalence of ISNA compared to stents with angulation ≤29° [18 (18.4%) *vs.* 23 (9.9%), P=0.032]. There is no difference in distribution of side branch between two groups. Angiographic findings are shown in *Table 2*.

The neointimal characteristics and ISNA distribution analyzed by OCT imaging

Two observers showed a high consistency in measurement results (r>0.9; P<0.001). Finally, 331 patients were included in OCT analyses, of which 41 patients with ISNA. OCT results showed that mean neointimal thickness (0.16 *vs.* 0.08 mm, P<0.001) and mean neointimal area (1.32 *vs.* 0.72 mm^2, P<0.001) in the patients with ISNA was increased significantly compared with those in without ISNA.

In stents with curves, the ISNA seemed to more often occurred at the inner curvature than at the outer curvature (77.8% *vs.* 22.2%, P=0.018). The relationship between ISNA location and the side of the branch was also evaluated (*Figure 2*). Twenty-seven (65.9%) stent segments in the ISNA group were with the relevant branch. If ISNA occurred in the bifurcation, it was more often found on the

Table 1 Patient characteristics

Characteristics	With ISNA (N=41)	Without ISNA (N=290)	P value
Age, years	57.9±13.6	58.5±9.6	0.863
Gender, male, n (%)	28 (77.8)	204 (70.3)	0.353
Hypertension, n (%)	22 (61.1)	179 (61.7)	0.943
Hyperlipidemia, n (%)	9 (25.0)	81(27.9)	0.711
Diabetes, n (%)	10 (27.8)	112 (38.6)	0.205
Smoking, n (%)	15 (41.7)	130 (44.8)	0.719
FBG, mmol/L	5.85 (5.25–7.07)	5.48 (4.94–6.46)	0.098
TC, mg/dL	152.5 (132.8–189.2)	147.1 (128.2–177.6)	0.894
TG, mg/dL	131.1 (113.5–198.0)	127.6 (95.9–169.0)	0.222
HDL, mg/dL	43.2 (37.8–49.8)	44.8 (38.2–54.4)	0.321
LDL, mg/dL	78.8±29.7	76.4±27.8	0.670
Stent diameter, mm	2.88 (2.50–3.50)	3.00 (2.50–3.00)	0.977
Stent length, mm	29.0 (18.0–36.0)	28.0 (18.0–33.0)	0.313

ISNA, in-stent neoatherosclerosis; FBG, fasting blood glucose; TC, total cholesterol; TG, triacylglycerol; HDL, high-density lipoprotein-cholesterol; HDL, low-density lipoprotein-cholesterol.

opposite side of the branch compared with on the same side of the branch [21 (77.8%) *vs.* 6 (22.2%), P=0.004]. There was no significant difference in the distribution of ISNA at the proximal and distal branch or curve (P>0.05) (*Table 3*).

Discussion

A growing number of studies have reported the presence of ISNA in BMS and DES (2,3,12). And the ISNA has been identified as an additional entity that could be related to the development of very late in-stent restenosis and very late stent thrombosis (3). The mechanisms of ISNA formation are multifactorial. Most of previous studies were focused on the molecular mechanism, few know about the distribution of ISNA. This is the first OCT study investigating the distribution of ISNA and the relationship between ISNA location and stent curvature as well as the side of the branch after SES implantation.

In this study, the mean duration of follow-up of patients with ISNA was 19 months, which was similar to the histology findings of Nakazawa *et al.* (3). The mean neointimal thickness in the ISNA group was much thicker than that in the NSNA group. This result was also in accordance with data from previous OCT studies (13).

We focused mainly on the distribution of ISNA using OCT. As previous studies showed that coronary lesions do not develop randomly, but instead localize at certain selected sites in the arterial tree (e.g., major bifurcations, T-junctions), which leaves the flow-divider free of lesions, as well as along the inner wall of curved segments (14,15). This phenomenon may also found on formation of ISNA. Combining coronary angiography and OCT, we found that ISNA occurred more often at the inner curvature than in the outer curvature, and was found more often at the opposite side of the branch compared with the same side of the branch. This distribution of ISNA may due to the difference of shear stress on the vessel wall.

Although the entire vasculature is exposed to the atherogenic effect of systemic risk factors, atherosclerotic lesions form at specific regions of the arterial tree where there is disturbed flow (14). Low endothelial shear stress (ESS) in particular, critically affects the formation, progression, and heterogeneity of atherosclerotic plaque (16). Flow velocity patterns and the concomitant shear stress profiles, depend on the velocity profile itself, blood viscosity, lumen diameter and vessel geometry. Blood flow is laminar in most cases, which means the blood flows in parallel layers, without intersecting. At a curvature, secondary flow can occur, meaning that flow is moving perpendicular to the flow direction. This is still considered laminar flow as

Table 2 Quantitative coronary angiography

Characteristics	With ISNA (N=41)	Without ISNA (N=290)	P value
Stent location in different vessels, n (%)			0.365
LAD	17 (41.5)	146 (52.1)	
LCX	8 (19.5)	53 (18.9)	
RCA	16 (39.0)	81 (28.9)	
Stent location in LAD, n (%)			0.793
LAD-P	6 (35.3)	43 (27.6)	
LAD-M	9 (52.9)	94 (60.3)	
LAD-D	2 (11.8)	19 (12.2)	
Stent location in LCX, n (%)			0.609
LCX-P	3 (37.5)	25 (47.2)	
LCX-D	5 (62.5)	28 (52.8)	
Stent location in RCA, n (%)			0.307
RCA-P	6 (37.5)	17 (21.0)	
RCA-M	7 (43.8)	38 (46.9)	
RCA-D	3 (18.8)	26 (32.1)	
Stent angulation >29°, n (%)	18 (43.9)	80 (27.6)	0.032
With branch, n (%)	27 (65.9)	179 (61.7)	0.610
RVD (mm)	2.90±0.31	2.98±0.37	0.178
MLD (mm)	2.24±0.36	2.52±0.41	<0.001
DS%	22.8±5.23	15.6±4.22	<0.001

ISNA, in-stent neoatherosclerosis; LAD, left anterior descending artery; LCX, left circumflex artery; RCA, right coronary artery; D, distant; M, middle; P, proximal; RVD, reference vessel diameter; MLD, minimal luminal diameter; DS%, percent diameter stenosis.

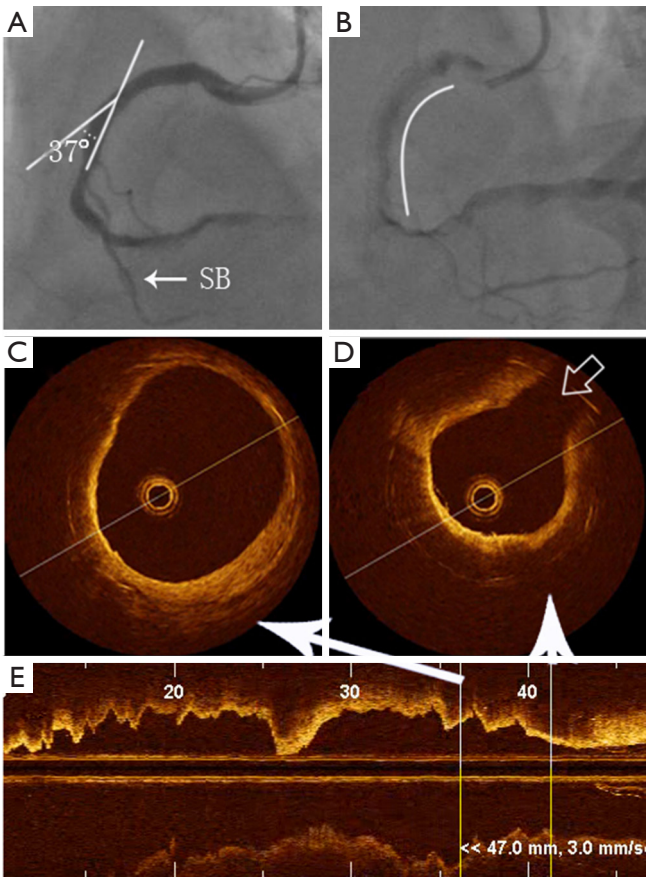

Figure 2 Localization of ISNA in relation to curvatures and bifurcations by OCT. (A) Angiography showing the vascular angle to be 37°; (B) the stent is in the middle of the RCA, the arc represents the stent length. The distance from the side-branch vessel to the stent edge is 3 mm (SB, side branch); (C,D) example of neoatherosclerosis by OCT, which is identified as a diffusely bordered, signal-poor region with overlying signal-rich homogenous bands. Gray arrow shows the location of the side branch; (E) OCT image shows the longitudinal axis of the cross-section of the blood vessel. ISNA, in-stent neoatherosclerosis; OCT, optical coherence tomography.

parallel flow layers are present. The peak velocity shifts to the outer curvature of the vessel, resulting in a higher shear stress at the outer curvature compared to the inner curvature (17). As a result, atherosclerotic plaque should prefer to form at inner curvature, as describing in our study. This result is in accordance with previous studies (18,19). The plaques at the outer curvature are prone to rupture. However, we did not observe rupture of ISNA in our study. The long term follow-up should be performed to evaluate the result of these plaques.

We also found that if ISNA occurred in a bifurcation site, it was more often found on the opposite side of the branch than on the same side of the branch. We also can find the role of EES in this phenomenon. As described previous, at bifurcations, secondary flow is present similar to flow patterns seen at curvatures, resulting in particle movement parallel and perpendicular to the vessel wall (17), a low ESS is formed on the opposite side of the branch. Therefore, Malek *et al.* suggested that atherogenesis preferentially involves the outer walls of vessel bifurcations (20). Although

Table 3 Distribution of ISNA

Stent (n=41)	N (%)
Stent angulation >29°	18 (43.9)
Curve proximal	10 (55.6)
Curve distal	8 (44.4)
P (curve proximal *vs*. distal)	0.637
Inner curvature	14 (77.8)
Outer curvature	4 (22.2)
P (inner curvature *vs*. outer curvature)	0.018
With branch	27 (65.9)
Branch-proximal	15 (52.2)
Branch-distal	12 (47.8)
P (branch-proximal *vs*. distal)	0.564
Branch-sameside	6 (22.2)
Branch-opposite	21 (77.8)
P (branch-sameside *vs*. opposite)	0.004

ISNA, in-stent neoatherosclerosis.

there may be different in molecular mechanism between ISNA and native plaque, the role of EES in both are same.

Limitation

This was a retrospective analysis. All patients' data was screened from our OCT database. There is a bias in patient selection. And the number of patients with ISNA was relatively small and the follow up time no long enough to evaluate the result of these ISNA. Furthermore, we can't measure the ESS, and interpretation of results was based on previous studies and inference. However, what we found in our study should be a hint for the studies in mechanism of ISNA formation.

Conclusions

In this study we have evaluated the localization of ISNA by OCT. We found that the localization of ISNA is related to vessel curvatures and bifurcations. ISNA occurs more often on the inner curvature and the opposite side of a branch. The ESS may play an important role on the formation of ISNA.

Acknowledgements

We gratefully acknowledge the valuable cooperation of Dr. Meng Sun (Statistical laboratory, Harbin Medical University) and Dr. Lulu Li (Department of Cardiology, the 2nd Affiliated Hospital of Harbin Medical University) in data statistics. We also gratefully acknowledge Dr. Xuefeng Ren, Dr. Huai Yu and Dr. Guang Yang (Department of Cardiology, the 2nd Affiliated Hospital of Harbin Medical University) for performing OCT imaging.

Funding: This work was supported by the Grants of the Natural Science Foundation of Heilongjiang (Grant Number: H2015005), the Fund of Health and Family Planning Commission of Heilongjiang Province (Grant Number: 2014-338) and the Heilongjiang Postdoctoral Fund (Grant number: LBH-Z15004).

Footnote

Conflicts of Interest: The authors have no conflicts of interest to declare.

Ethical Statement: This protocol was approved by the Harbin Medical University Ethics Committee (No. KY-2015-105), and all patients received statins and antiplatelet therapy during the follow-up period.

References

1. Karanasos A, Ligthart JM, Regar E. In-stent neoatherosclerosis: a cause of late stent thrombosis in a patient with "full metal jacket" 15 years after implantation: insights from optical coherence tomography. JACC Cardiovasc Interv 2012;5:799-800.
2. Kang SJ, Mintz GS, Akasaka T, et al. Optical coherence tomographic analysis of in-stent neoatherosclerosis after drug-eluting stent implantation. Circulation 2011;123:2954-63.
3. Nakazawa G, Otsuka F, Nakano M, et al. The pathology of neoatherosclerosis in human coronary implants bare-metal and drug-eluting stents. J Am Coll Cardiol 2011;57:1314-22.
4. Ali ZA, Roleder T, Narula J, et al. Increased thin-cap neoatheroma and periprocedural myocardial infarction in drug-eluting stent restenosis: multimodality intravascular imaging of drug-eluting and bare-metal stents. Circ Cardiovasc Interv 2013;6:507-17.
5. Whitbeck MG, Applegate RJ. Second generation drug-

eluting stents: a review of the everolimus-eluting platform. Clin Med Insights Cardiol 2013;7:115-26.
6. Lee SY, Hur SH, Lee SG, et al. Optical coherence tomographic observation of in-stent neoatherosclerosis in lesions with more than 50% neointimal area stenosis after second-generation drug-eluting stent implantation. Circ Cardiovasc Interv 2015;8:e001878.
7. Bourantas CV, Papafaklis MI, Kotsia A, et al. Effect of the endothelial shear stress patterns on neointimal proliferation following drug-eluting bioresorbable vascular scaffold implantation: an optical coherence tomography study. JACC Cardiovasc Interv 2014;7:315-24.
8. Lee SY, Shin DH, Mintz GS, et al. Optical coherence tomography-based evaluation of in-stent neoatherosclerosis in lesions with more than 50% neointimal cross-sectional area stenosis. EuroIntervention 2013;9:945-51.
9. Yonetsu T, Kato K, Kim SJ, et al. Predictors for neoatherosclerosis: a retrospective observational study from the optical coherence tomography registry. Circ Cardiovasc Imaging 2012;5:660-6.
10. Badak O, Schoenhagen P, Tsunoda T, et al. Characteristics of atherosclerotic plaque distribution in coronary artery bifurcations: an intravascular ultrasound analysis. Coron Artery Dis 2003;14:309-16.
11. Gonzalo N, Serruys PW, Barlis P, et al. Multi-modality intra-coronary plaque characterization: a pilot study. Int J Cardiol 2010;138:32-9.
12. Higo T, Ueda Y, Oyabu J, et al. Atherosclerotic and thrombogenic neointima formed over sirolimus drug-eluting stent: an angioscopic study. JACC Cardiovasc Imaging 2009;2:616-24.
13. Vergallo R, Yonetsu T, Uemura S, et al. Correlation between degree of neointimal hyperplasia and incidence and characteristics of neoatherosclerosis as assessed by optical coherence tomography. Am J Cardiol 2013;112:1315-21.
14. Chatzizisis YS, Coskun AU, Jonas M, et al. Role of endothelial shear stress in the natural history of coronary atherosclerosis and vascular remodeling: molecular, cellular, and vascular behavior. J Am Coll Cardiol 2007;49:2379-93.
15. Konta T, Bett JH. Patterns of coronary artery movement and the development of coronary atherosclerosis. Circ J 2003;67:846-50.
16. Samady H, Eshtehardi P, McDaniel MC, et al. Coronary artery wall shear stress is associated with progression and transformation of atherosclerotic plaque and arterial remodeling in patients with coronary artery disease. Circulation 2011;124:779-88.
17. Winkel LC, Hoogendoorn A, Xing R, et al. Animal models of surgically manipulated flow velocities to study shear stress-induced atherosclerosis. Atherosclerosis 2015;241:100-10.
18. Loree HM, Kamm RD, Stringfellow RG, et al. Effects of fibrous cap thickness on peak circumferential stress in model atherosclerotic vessels. Circ Res 1992;71:850-8.
19. Cecchi E, Giglioli C, Valente S, et al. Role of hemodynamic shear stress in cardiovascular disease. Atherosclerosis 2011;214:249-56.
20. Malek AM, Alper SL, Izumo S. Hemodynamic shear stress and its role in atherosclerosis. JAMA 1999;282:2035-42.

Cite this article as: Zou Y, Huang X, Feng L, Hou J, Xing L, Yu B. Localization of in-stent neoatherosclerosis in relation to curvatures and bifurcations after stenting. J Thorac Dis 2016;8(12):3530-3536. doi: 10.21037/jtd.2016.11.108

